ATS/Note/2011/094 TECH
CERN-BETA-BEAMS-Report- 2011-001

10.11.2011

Elena.Benedetto @cern.ch

Beta Beams Production Ring, Status Report

Benedetto, E

Beta Beams

Summary

This report presents the status of the first year studies on the Production ring, in the framework of the Beta BeamWork Package within EURONU. The ionization cooling, physics and efficiency, and the technological issues are here discussed.

November 2011

Beta Beams Production Ring, Status Report

Elena Benedetto

January 12, 2011
(revised: October 4, 2011)

Abstract

This report presents the status of the first year studies on the Production ring, in the framework of the Beta Beam Work Package within EURONU. The ionization cooling, physics and efficiency, and the technological issues are here discussed.

Contents

1 Introduction

The Beta Beam concept foresees the production of pure electron neutrinos and anti-neutrinos for oscillation experiments from the beta-decay of suitable isotopes [1]. Such a facility could be advantageously placed at CERN making use of the Proton Synchrotron(PS) and Super Proton Synchrotron (SPS) for accelerating the radioactive ions to a Lorentz γ_r of 100. Within EURISOL [2] under the European Framework Program 6 (FP6), the ^{6}He and ^{18}Ne as neutrino and anti-neutrino emitters have been studied. Intense beams would be produced using the so-called Isotope-Separation On Line (ISOL) method, transported to an Electron Cyclotron Resonance (ECR) source, accelerated though a Rapid Cycling Synchrotron, then in the PS, SPS and finally stored in a Decay Ring, as shown in the schematics in Fig. 1, left. For an optimal sensitivity of the Beta Beam facility to the θ_{13} angle and CP violating phase, a total throughput of $1.1\,10^{19}$ neutrinos and $2.9\,10^{19}$ anti-neutrinos was generally assumed over a running period of 10 years (200 d/y, 50% efficiency). In turn, a top-down approach results in the need for production of about $3.3\,10^{13}$ ^{6}He radioactive atoms and $2.1\,10^{13}$ ^{18}Ne atoms per second, taking into account efficiency coefficients along the accelerator chain [2].

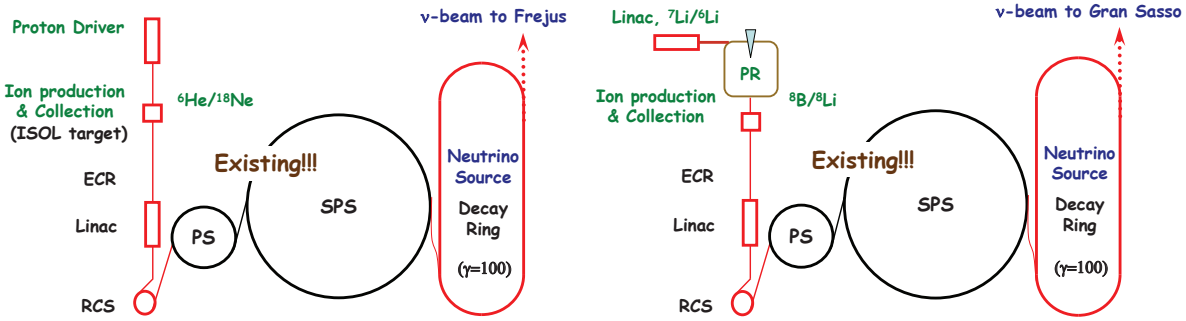

Figure 1: Beta Beam complex. Left: FP6-EURISOL proposal (^{6}He and ^{18}Ne). Right: FP7-EURONU proposal (^{8}Li and ^{8}B).

Since at the end of FP6 Program there was a shortfall in the ^{18}Ne production, the FP7 Program EUROnu Beta Beam Work Package [3] is considering an additional new pair of isotopes, namely ^{8}Li and ^{8}B, as anti-neutrino and neutrino emitters. The main changes to the Beta Beam layout (see Fig. 1, right) are a longer baseline for the detector, which would also allow mass hierarchy measurements, and a new production method with a compact storage ring equipped with an internal target [4]. Indeed, due to the higher energy of the (anti-)neutrinos emitted by ^{8}B and ^{8}Li, the detector needs to be placed at $\sim$ 700 km (e.g. Gran Sasso or Canfranc) instead of the 130 km of Frejus, in order to detect the first oscillation peak. The cross section is larger for higher energy neutrinos, but the incoming flux is reduced due to the solid angle opening. The sensitivity studies in [5] indicate that for ^{8}Li and ^{8}B a factor 5 more intensity is required, which corresponds to $\sim 10^{14}$ radioactive ions produced per second.

Concerning the new production scheme, [4] proposes a compact synchrotron in which a 25 MeV Lithium ion beam circulates and interacts with a D or ^{3}He supersonic gas-jet target, to exploit the ^{7}Li(d,p)^{8}Li and ^{6}Li(^{3}He,n)^{8}B reaction channels. The radioactive isotopes, produced at every passage through the target, are collected by a special device which stops and transports them to the charge-breeder ECR-source by a diffusion/effusion ISOL-like mechanism, for further acceleration through the Beta Beam complex.

The stored beam is expected to survive for several thousands of turns, corresponding to the production characteristic time for the target thickness proposed in [4] and according to this scheme, the ionization cooling [6, 7] provided by the target itself and a suitable RF system would be sufficient to compensate for Multiple Coulomb Scattering and energy straggling.

The first part of the report introduces the ionization cooling mechanism and gives an estimation for the cooling potential for a Beta Beam Production Ring. The lattice design, subject of the work of [8], and the ring parameters are then reported. Finally, the tracking simulations work [9] and the results in terms of emittance evolution and beam losses are presented. In the second part, technological solutions and challenges for the production ring, as originally proposed in [4], are discussed, with special attention to the requirements for the gas-jet target, the stable Li source, the RF cavity and the vacuum issues. Finally, when the feasibility of the proposal cannot be easily demonstrated and/or when we think it could be an interesting option to be considered, alternative solutions are identified and discussed.

2 Description of the Production Ring and ionization cooling

2.1 The Production Ring

In order to produce ^{8}Li and ^{8}B from the reactions ^{7}Li(d,p)^{8}Li and ^{6}Li(^{3}He,n)^{8}B, [4] proposes to use of a compact ring in which a Lithium beam is stored and interacts with a D or ^{3}He supersonic gas-jet target. The small synchrotron has a circumference of about 10 m and the beams kinetic energy is 25 MeV, giving a relativistic beta of about $\beta_r \sim 0.1$. The ions are injected as Li^{1+} at the target location via a charge-exchange method where the target itself is acting as a charge stripper. At 25 MeV, the circulating beam is fully stripped. The radioactive isotopes, produced at every passage through the target, are emitted in a narrow angular cone of about 8^o [10]. A special collection device [11] stops them and transports them to the charge-breeder ECR-source, for further acceleration through the Beta Beam complex.

Due to the interaction with the target, the stored beam suffers of longitudinal and transverse emittance blow-up, induced by Multiple Coulomb Scattering and energy straggling. The beam degradation is kept under control with the ionization cooling mechanism provided by the target itself and a suitable RF system.

2.1.1 Circulating beam

The number of particles N circulating in the ring is given by the following equation:

$$\frac{dN}{dt} = -\frac{1}{\tau}N + I_{source} \tag{1}$$

Following Ref. [4], in order to produce 10^{14} radioactive isotopes per second, the ^{7}Li ion source has to provide $I_{source} = 160\mu\text{A} = 10^{15}$ ions/s. Being $\tau = 10^4$ turns $/f_{rev} = 3$ ms the nuclear lifetime, after a ∼few ms transitory there will be $\sim 10^{12}$ ^{7}Li particles circulating in the ring. For the ^{8}B production, since the nuclear cross-section is a factor 10 smaller, these quantities have to be increased by the same factor.

2.1.2 Internal target

The circulating Lithium beam is interacting with the production target at every passage in the ring. According to [4], for the energies of interest, the cross-section for the nuclear reaction ^{7}Li(d,p)^{8}Li is about 100 mbarn, while for the ^{6}Li(^{3}He,n)^{8}B reaction it is about 10 mbarn (see also [12, 13]).

The total cross-section, thus the sum of the nuclear elastic and inelastic reaction cross-sections, which causes the ejection of the particle from the beam, is typically of 1 barn for both ^{6}Li and ^{7}Li nuclei and, assuming a target thickness $t = 0.277$ mg/cm^2 [4], this corresponds to a nuclear beam lifetime of about $n \sim 10^4$ turns.

The blow-up due to Multiple Coulomb Scattering is evaluated using the Moliere rms angle equation:

$$\theta_c = \sqrt{\langle\theta^2\rangle} = \frac{14.1MeV}{\beta_r cp} z\sqrt{\frac{t}{\chi_0}}\left[1 + 0.038\ln\frac{t}{\chi_0}\right] \tag{2}$$

where $\beta_r c$, γ_r, p and z are the velocity, relativistic mass factor, momentum and charge of the incident ion and χ_0 is the radiation length.

The mean energy lost at the target is estimated via the Bethe–Bloch formula [14]:

$$\Delta E_{BB} = \left\langle\frac{dE_L}{dx}\right\rangle t = Kz^2\frac{Z}{A}\frac{1}{\beta_r^2}\left[\frac{1}{2}\ln\frac{2m_e c^2\beta_r^2\gamma_r^2 T_{\max}}{I^2} - \beta_r^2 - \frac{1}{2}\delta(\beta_r\gamma_r)\right]t \tag{3}$$

where A, Z and I are the target atomic mass, charge and mean excitation energy. The quantity

$$T_{max} = \frac{2m_e c^2\beta_r^2\gamma_r^2}{1 + 2\gamma_r m_e/M + (m_e/M)^2} \tag{4}$$

is the maximum kinetic energy which can be imparted to a free electron in a single collision, with m_e the electron mass and M the mass of the incident particle, and $K = 4\pi N_A r_e^2 m_e c^2$ is a constant, being r_e the classical electron radius and N_A the Avogadro's number.

For a target thickness of $t = 0.277$ mg/cm^2 [4], the average energy lost by a Lithium ion is 300 keV, value that needs to be restored by a strong RF system.

Energy fluctuations are assumed to have a Gaussian distribution, with an r.m.s. width of about $\sqrt{\langle \delta_{rms}^2 \rangle} = 15$ keV, as from Table 1 in [4].

Losses due to single large-scattering events [15] and by Intra-Beam Scattering are for the time being not included in the computations.

2.2 Ionization Cooling

The ionization cooling [6] is recently receiving large attention for the fast cooling of muons for a Neutrino Factory or a Muon Collider [7]. It is based on the principle that a beam traversing a material looses energy and only its longitudinal component is recovered in the RF cavities, with the net effect of a transverse emittance shrinking, as sketched in Fig. 2.

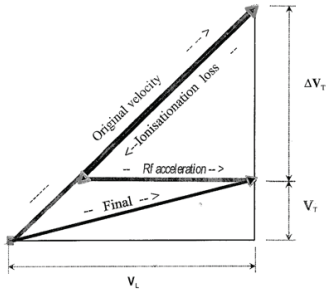

Figure 2: The principle of transverse ionization cooling [16].

In analogy to synchrotron radiation damping, one can introduce [7] partition numbers, whose sum is invariant, to characterize the cooling rates in the three planes and define equilibrium emittances from the balance between the cooling terms and the heating ones.

The challenge of applying ionization cooling for low-energy ions resides in the strongly negative slope of the Bethe-Bloch formula [14] for the energies of interest. In particular, $(\partial E_{loss}/\partial p) < 0$ means that for an increase of particle momentum, the energy losses in the material becomes weaker, thus causing strong heating, instead of cooling, in the longitudinal plane. Longitudinal cooling can be achieved by introducing coupling with the horizontal plane via the dispersion and by using a wedge-shaped absorber in a dispersive region, but since the sum of the partition numbers is a constant (and in this case only slightly positive [17]), one can achieve longitudinal cooling only at expenses of the transverse one.

Following the derivation of [7], the equations for the normalized horizontal and vertical emittances $\varepsilon_{N,i} = \beta_r \gamma_r \varepsilon_i$, with $i = x, y$, are:

$$\frac{d\varepsilon_{N,x}}{ds} = -J_x \frac{1}{p}\frac{dp}{ds}\varepsilon_{N,x} + \beta_r \gamma_r \frac{\beta_x}{2}\frac{d\left\langle \theta_c^2 \right\rangle}{ds} \tag{5}$$

$$\frac{d\varepsilon_{N,y}}{ds} = -J_y \frac{1}{p}\frac{dp}{ds}\varepsilon_{N,y} + \beta_r \gamma_r \frac{\beta_y}{2}\frac{d\left\langle \theta_c^2 \right\rangle}{ds} \tag{6}$$

The first term on the right side of the equations is the energy-loss cooling term. It is characterized by the partition numbers J_x and J_y, which, in case there is no coupling between the planes, are:

$$J_x = J_y = 1 \tag{7}$$

and it is proportional to the relative momentum losses at the target, which can be expressed in terms of kinetic energy E_c and energy losses $\left\langle \frac{dE_L}{ds} \right\rangle$ from the Bethe-Bloch formula [14] as:

$$\frac{1}{p}\frac{dp}{ds} = \frac{\gamma_r}{\gamma_r + 1}\frac{1}{E_c}\left\langle \frac{dE_L}{ds} \right\rangle \tag{8}$$

The second term in the Eqs. 5, 6 represents the blow-up term due to Multiple Coulomb Scattering, where $\left\langle \theta_c^2 \right\rangle$ is the rms multiple scattering angle, evaluated from Eq. 2, and $\beta_{x,y}$ are the horizontal and vertical betatron functions at the target location.

For the target thickness $t = 0.277$ mg/cm^2 [4], which induces an average energy lost at the target of $\Delta E_{BB} = \int_0^t \left\langle \frac{dE_L}{ds} \right\rangle ds = 0.3$ MeV, it follows from Eqs. 5, 6 and 8 that the damping times in the transverse plane is:

$$\tau_i = J_i \left(\int_0^t \frac{1}{p}\frac{dp}{ds} ds \right)^{-1} = 167 \text{ turns}, \quad i = x, y \tag{9}$$

and the equilibrium emittances are:

$$\varepsilon_i = \frac{\varepsilon_{N,i}}{\beta_r \gamma_r} = \tau_i \int_0^t \frac{\beta_i}{2}\frac{d\left\langle \theta^2 \right\rangle}{ds} ds = \beta_i \times 33.5 \text{ mm mrad}, \quad i = x, y \tag{10}$$

for an r.m.s. multiple scattering angle of $\sqrt{\langle \theta^2 \rangle} = 6.35 \times 10^{-4}$.

Concerning the longitudinal plane, the equation for the emittance evolution is [7]:

$$\frac{d\varepsilon_{N,l}}{ds} = -J_l \frac{1}{p}\frac{dp}{ds}\varepsilon_{N,l} + \beta_r \gamma_r \frac{\beta_l}{2}\frac{d\left\langle \delta_{rms}^2 \right\rangle}{ds} \tag{11}$$

where J_l is the longitudinal partition number and $\left\langle \delta_{rms}^2 \right\rangle$ is the r.m.s. energy straggling (assuming a Gaussian fluctuation distribution).

β_l is a longitudinal focusing function defined as:

$$\beta_l^2 \equiv \frac{\left\langle z^2 \right\rangle}{\left\langle \delta^2 \right\rangle} = \frac{\beta_r^2 p\, c\, C\, \lambda_{RF}\, \alpha_c}{2\pi z e V_{RF} \sin \phi_s} \tag{12}$$

where C is the ring circumference, α_c the momentum compaction, ze the particle charge, λ_{RF} and V_{RF} the RF wavelength and RF voltage and ϕ_s the synchronous RF phase.

One should note that the longitudinal partition number J_l, which is proportional to the rate of change of the energy lost at the target with respect to the change in energy, $\frac{\partial}{\partial E}\left\langle \frac{dE_L}{ds} \right\rangle$

(i.e. the slope of the Bethe-Bloch curve), is strongly negative for the energies of interest and therefore in this plane there is no ionization cooling, but heating:

$$J_l = \frac{\frac{\partial}{\partial E}\left\langle \frac{dE_L}{ds} \right\rangle}{\frac{1}{p}\frac{dp}{ds}} = \begin{cases} -1.6 \text{ for } {}^6\text{Li} \\ -1.99 \text{ for } {}^7\text{Li} \end{cases} \tag{13}$$

In order to achieve cooling in the longitudinal plane, it is necessary to introduce coupling with the horizontal plane in the region of the target via the dispersion and to introduce a wedge shape for the target itself, so that the thickness $\rho(x)$ seen by a particle depends on its horizontal offset x (i.e. on its momentum offset) and the partition numbers become:

$$J_l \rightarrow J_l + D_x \frac{1}{\rho_0}\frac{d\rho(x)}{dx} \tag{14}$$

$$J_x \rightarrow J_x - D_x \frac{1}{\rho_0}\frac{d\rho(x)}{dx} \tag{15}$$

$$J_y \rightarrow J_y \text{ (as there is no x–y coupling)} \tag{16}$$

The total cooling power, which is the sum of the partition numbers, cannot be changed, however it can be transferred from one plane to the other via the dispersion (x–z coupling) and other coupling mechanisms.

The sum of the partition numbers, as it should always be the same, can be computed for the case of no coupling (Eqs. 7, 13):

$$\sum J_i = 1 + 1 + \frac{\frac{\partial}{\partial E}\left(\frac{dE_L}{ds}\right)}{\frac{1}{p}\frac{dp}{ds}} = \begin{cases} 0.4 \text{ for } {}^6\text{Li} \\ 0.01 \text{ for } {}^7\text{Li} \end{cases} \tag{17}$$

The result shows that for the case of the Production Ring for Beta Beam isotopes, using a ^{7}Li or ^{6}Li beam at $\sim$ 25 MeV impinging on a D or ^{3}He target, the cooling efficiency is very low, almost zero. This depends on the slope of the Bethe-Bloch equation and could be improved only by changing the beam energy, on which there is not much freedom since it is set to optimize the production cross-section.

The practical meaning, for the Production Ring application, is that there is a very small margin for cooling and only in the case of perfect emittance exchange, achieved by coupling the longitudinal plane both with the horizontal and with the vertical, it will be possible to keep the beam size under control, as already pointed out in [17].

3 Tracking simulations

3.1 The proposed lattice

The optics of the 12m–long production ring for the 25 MeV ^{7}Li ions (to produce ^{8}Li isotopes) is shown in Fig. 3 and the design is well documented in [8]. The ring has a two-fold

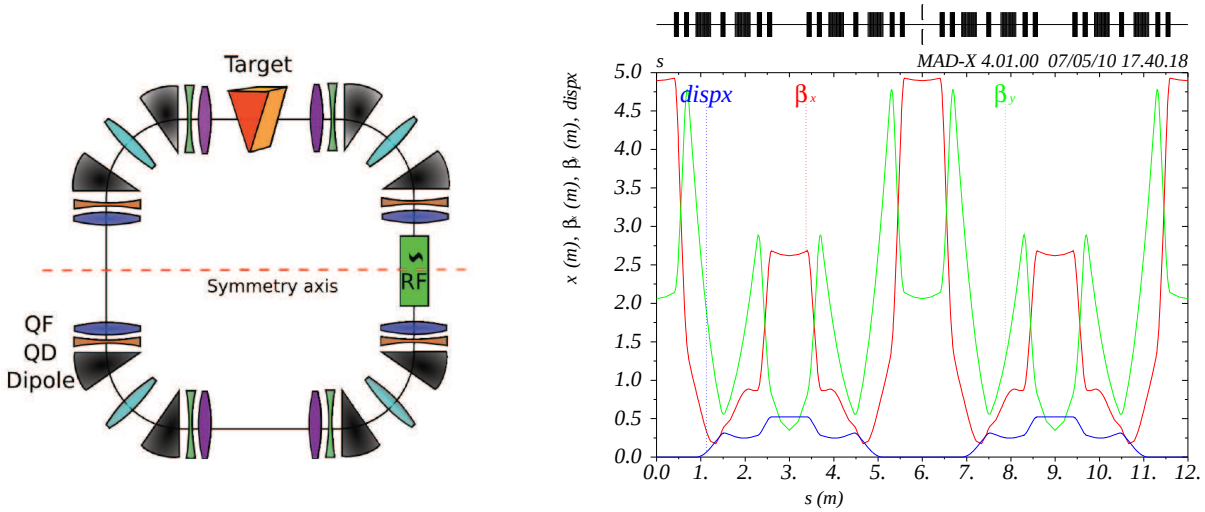

Figure 3: Sketch of the Production Ring and Twiss parameters [8].

symmetry: two of the straight sections have zero dispersion, in order to accommodate the RF cavity(ies), the other two, instead, have an horizontal dispersion of 50 cm, as required by the specifications for the production target, which will be installed in one of them. Table 1 summarizes the ring parameters.

For the following simulations, the working point of $(2.58, 1.63)$ has been choosen. The horizontal β_x is for the moment of about 2.6 m at the target and leads to important beam blow-up due to Multiple Coulomb Scattering.

For particles with "large" momentum offset (i.e. of the order of 1%), the large negative chromaticity may induce resonance crossing and losses. A first attempt to include sextupoles in the lattice to compensate the chromaticity led to dynamic aperture problems. A trade-off between the increase in tune spread and the reduction in dynamic aperture has to be found. Moreover, as shown in Fig 4, a large second order dispersion in the straigth sections leads to a non-zero dispersion in the RF cavity for particles with a 1% momentum offset and to a 10% difference in the cooling section, which may need to be taken into account.

This lattice, which still needs to be tuned for optimizing the cooling efficiency, is used to set-up tracking simulations and for identifying the parameters to reduce the blow-up [18].

3.2 The code SixTrack

SixTrack [19] is a fully 6D, single-particle tracking code, based on high order truncation of Taylor expansion, which is widely used at CERN for dynamic aperture studies and for collimation. It can read the lattice directly form a MADX-PTC special output file, including higher order multipole components. The collimation version [20] has the possibility to track

Table 1: Production ring parameters.

Particle		^{7}Li
Kinetic energy	E_c	25 MeV
Relativistic mass factor	γ_r	1.00383
Beam rigidity	$B\rho$	0.636 T m
Circumference	C	12 m
Revolution frequency	f_{rev}	2.18 MHz
Transition γ	γ_t	3.58
Tune	$Q_{x,y}$	2.58, 1.63
Natural chromaticity	$Q'_{x,y}$	-3.67, -3.58
β @ target	$\beta^*_{x,y}$	2.62 m, 0.35 m
Dispersion @ target	$D^*_{x,y}$	0.523 m, 0 m
Target thickness	t_0	0.27 mg/cm^2
Target thickness	n_t	10^{19} atoms/cm^2
Energy losses @ target	E_{BB}	300 keV

an initial particle distribution and to model the beam evolution in special elements such as collimators.

3.2.1 Code modifications

The production target has been implemented in the code as a special element and the interaction with matter modeled by simple analytical formulas. The energy lost by a particle traversing a target is a random value from a Gaussian distribution, with the mean given by the Bethe-Bloch formula (Eq. 3), and the rms spread (energy straggling) proportional to the target thickness and hard-coded with the value from Table 1 in [4]. For the Multiple Coulomb Scattering, Eq. 2 is used.

Since SixTrack can only deal with protons, an equivalent proton beam is tracked, with the same rigidity ($B\rho$) and the same momentum $\Delta p_{RF}/p$ recovered at the RF-cavity. Before the interaction with the target, the proton energy is converted to the ^{7}Li equivalent and then back again after the target [8]. The equivalent proton energy is 19 MeV and the energy recovered at the RF cavity is $\Delta E_{RF} \sim 0.22$ MeV for the reference particle. The RF voltage and synchrotron phase, for an harmonic number $h = 1$, have been set to $V = 860.6$ kV and $\phi_s = 15^o$, from considerations of bucket height, but this can be further tuned.

Furthermore, a few beam diagnostics have been included in SixTrack, e.g. the possibility to have the turn by turn rms emittance evolution in the three planes.

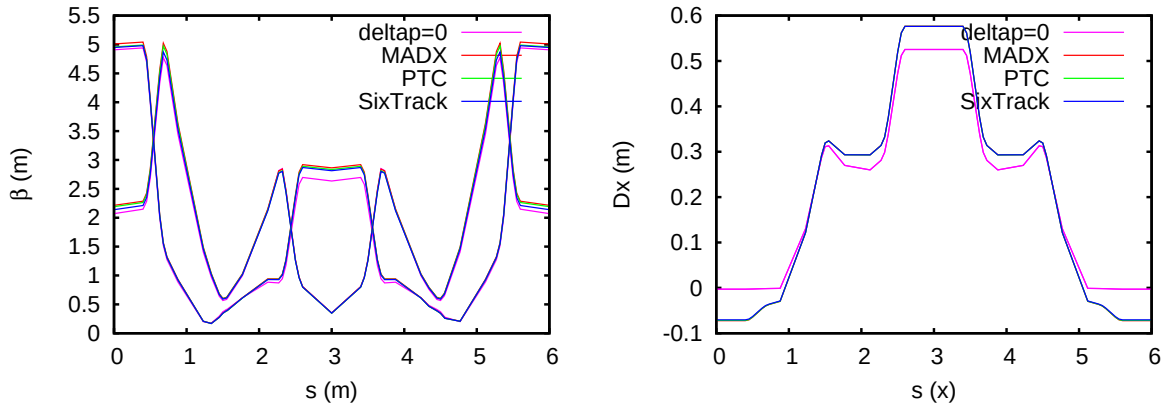

Figure 4: Horizontal and vertical beta functions (left) and dispersion (right) for a particle with a 1% momentum offset, compared to the reference particle. Different lines correspond to the different codes.

3.2.2 Comparison with MADX-PTC and the effect of momentum offset

Since SixTrack is mainly used for LHC tracking and, since there is not much experience with low energy machines, it was necessary to perform a benchmark with MADX and PTC. Figure 4 shows the beta functions and the dispersion for one half of the ring, for a momentum offset of 1%. Even for this "large" momentum offset, both MADX and SixTrack, which is using a truncated Taylor expansion, are in very good agreement with PTC, which is using the exact Hamiltonian. As it was previously mentioned, from these plots one can also note that the optics differences between a particle with the nominal energy and one with a 1% momentum offset are not negligeble, especially for what concerns the dispersion.

3.3 Simulations with a rectangular target

Figure 5 (left) shows the transverse and longitudinal beam evolution in the case of a rectangular-section target (zero wedge angle). One would like to see cooling in the horizontal and vertical plane and blow-up in the momentum spread.

Indeed, the momentum spread is increasing (blue curve) and generating important beam losses when it becomes larger then a few 10^{-2}. As shown in Fig. 5 (right), losses occur in the horizontal plane in the two high dispersion regions, for positive displacements, when the particles hit the aperture which is set to $a = 10$ cm.

From Fig. 5, it is however not clear whether cooling is reached in the transverse plane, as losses occurs for an aperture set to $a = 10$ cm (half size). The red curves in Fig. 6 shows the same case for zero wedge-angle, but assuming a larger aperture of the beam pipe, $a = 30$ cm. In these simulations, it is more evident that cooling occur for the first 300 turns, but when the momentum spread goes above 2%, there is a sudden change in the slope of the emittance

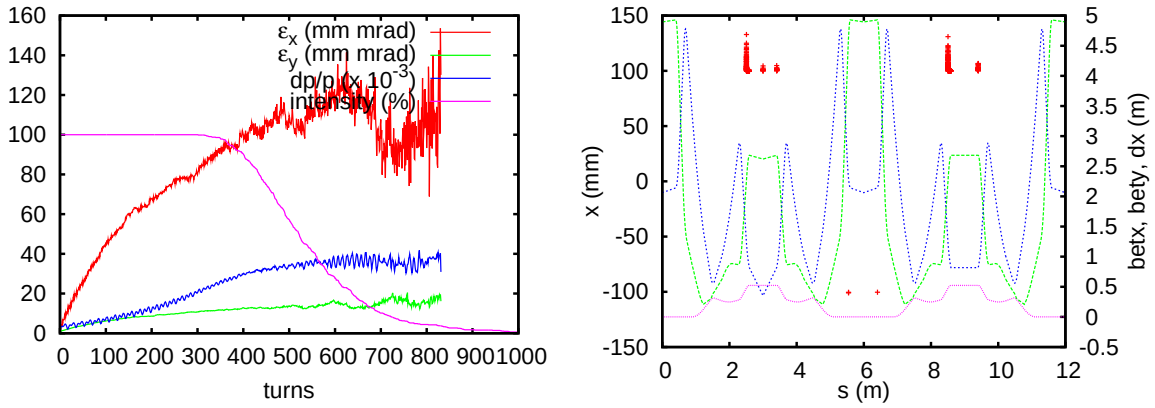

Figure 5: Left: Horizontal and vertical emittance, momentum spread and intensity evolution in case of a rectangular target. Right: Horizontal coordinate of lost particles. The half aperture is $a = 10$ cm.

evolution.

The emittance blow-up for large momentum spread has two explanations: first of all, it is due to the large, non-corrected natural chromaticity which leads to values of $\Delta Q \sim 0.8$, for a $\Delta p/p = 2 \times 10^{-2}$, and induces (integer) resonance crossing. Moreover, for the horizontal plane, the large second-order dispersion at the place where the emittance is computed generates an artificial emittance increase due to particles with non-zero dispersion whose invariant is not correctly evaluated.

If one restricts the analysis to the first 300 turns, the values found in the simulations are in agreement with the analytical estimations for the transverse equilibrium emittances (Eq. 10) of $\varepsilon_x = 87.7$ mm mrad in the horizontal plane and $\varepsilon_y = 11.7$ mm mrad in the vertical. Also the cooling time is of the order of the predicted 167 turns (Eq. 9).

In order to keep the momentum spread blow-up under control, a non-zero wedge angle for the target should be introduced.

3.4 The choice of wedge-angle

A wedge-shaped target in a dispersive region is used to transfer the cooling from the horizontal to the longitudinal plane. By linearizing the Bethe-Bloch formula, with respect to the target thickness variation Δt and the particle energy offset ΔE, one obtains:

$$E_{BB}(t, E_c) \approx \left.\frac{dE}{ds}\right|_{E_{c0}} t_0 + \left.\frac{dE}{ds}\right|_{E_{c0}} \Delta t + \left.\frac{\partial\left(\frac{dE}{ds}\right)}{\partial E_c}\right|_{E_{c0}} t_0\, \Delta E_c$$

The first term is the mean energy lost by a beam of nominal energy E_{c0}, traversing a target of uniform thickness t_0, and it is the energy recovered in the RF-cavity by the synchronous

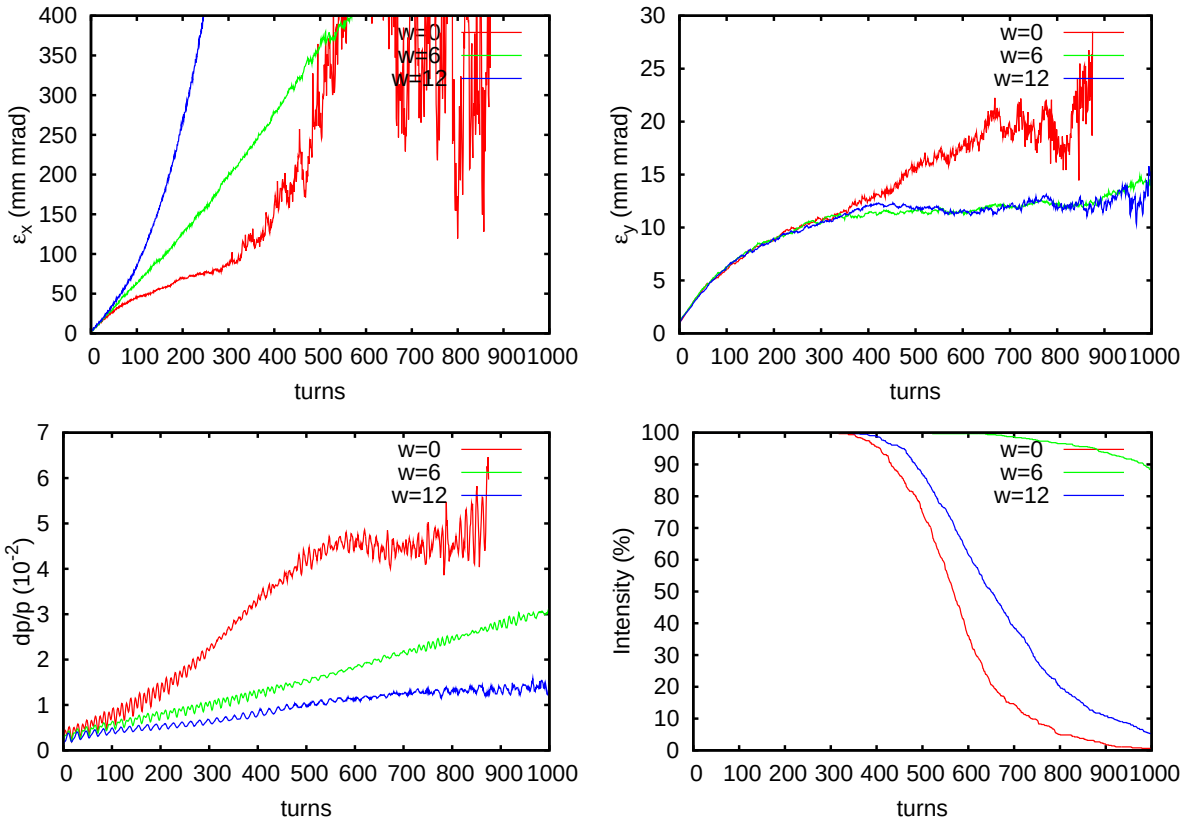

Figure 6: Emittances, rms momentum spread and beam intensity evolution for different target wedge angles. The aperture is $a = 30$ cm.

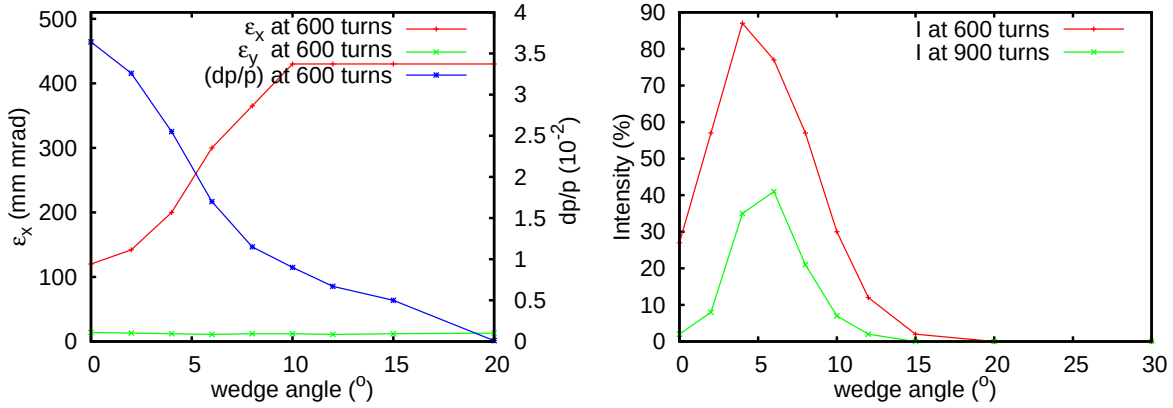

Figure 7: Left: Horizontal and vertical emittance and momentum spread after 600 turns as a function of the wedge angle. Right: Beam intensity after 600 and 900 turns. The aperture is $a = 10$ cm.

particle. The second and third terms both depend on the particle momentum offset ($\Delta p/p$), since it is:

$$\Delta E_c = E_c \, \frac{\gamma_r + 1}{\gamma_r} \, \frac{\Delta p}{p} \tag{18}$$

$$\Delta t = 2\,\rho \, \tan\frac{w}{2} \, \Delta x = 2\,\rho \, \tan\frac{w}{2} \, D^* \frac{\Delta p}{p} \tag{19}$$

where ρ is the target density, w is the angle of the wedge and Δx is the horizontal offset, induced by the dispersion D^* at the target.

By playing with the dispersion and the wedge-angle it is possible to compensate for the difference in mean loss value due to different particle energy and, in particular, to fully compensate for the losses dependence on the momentum offset if:

$$D^* \tan\frac{w}{2} = \frac{1}{2\rho} \left(\frac{dE}{ds}\right)^{-1}_{E_{c0}} \frac{\gamma_r + 1}{\gamma_r} \, \frac{\partial}{\partial E_c} \left(\frac{dE}{ds}\right)\Big|_{E_{c0}} t_0 \, E_c$$

The angle necessary to keep a constant momentum spread, thus to have no blow-up in the longitudinal plane, is $w = 15^o$, but, if one would chose this value, the blow-up in the horizontal plane would be too large and would lead to losses comparable to the zero-wedge case (see Fig. 6, bottom-right). Indeed, a $w = 6^o$ angle is the best compromise between the blow-up in the horizontal and longitudinal planes.

Figure 6 shows the transverse emittances, momentum spread and beam intensity for three different wedge angles. The beam pipe aperture has been set to $a = 30$ cm. For a $w = 6^o$ angle, the momentum spread increase is smaller than in the case of a rectangular target ($w = 0^o$), but this is obtained at the expense of a more important horizontal blow-up. In the vertical plane the cooling is the same as before, since there is no coupling. Increasing the wedge angle to 12^o leads again to strong losses, due to the uncontrolled horizontal blow-up.

Figure 7 shows the beam intensity, transverse emittances and longitudinal blow-up as a function of the wedge angle. The aperture has been set back again to $a = 10$ cm, which is a most realistic value. Even for the best case ($w = 6^o$), after 900 turns 60% of the beam is lost in the machine. This has to be compared to the expected production rate, which generates a decrease of the circulating beam with a caracteristic time of $\sim 10^4$ turns. This results can be improved by minimizing the horizontal beta function value at the target position and by introducing coupling with the vertical dimension, to share the cooling power in the three planes.

4 Technical solutions and challenges

In the following we discuss the outcome of a preliminary investigation about possible technical issues and solutions.

4.1 Primary ions source

According to [4], for the energies of interest for the ^{6}Li and ^{7}Li nuclei, the total cross-section is of the order of 1 barn. For the nuclear reaction ^{7}Li(d,p)^{8}Li, the cross section is about 100 mbarn at 25 MeV [12, 13], meaning that 10% of the interacting particles will produce a useful isotope. Therefore, in order to reach the 10^{14}/s radioactive-isotope flux from the production ring, as required from physics, one would need 10^{15}/s ^{7}Li particles injected. Assuming 100% transmission efficiency in the linac, this corresponds to 160 μA from the ^{7}Li source.

Existing ECRIS only reach $\sim 30\mu$A [21, 22], e.g. the high temperature oven in GSI [23] produces an operational ion current of 30 μA (maximum intensity over short periods goes up to 70 μA).The source is working in CW, since Lithium is too light for afterglow mode [21]. The transmission efficiency of a linac, not optimized for Li ions, is of order of 30% but it can be increased if a dedicated linac is built.

The primary ion intensity is not considered to be a show-stopper for the ^{8}Li production, since several sources could be added in parallel to feed the linac, and/or R&D has to be pushed.

For the ^{6}Li(^{3}He,n)^{8}B reaction, the cross section is about 10 mbarn, thus a factor 10 more intensity should be provided from the source, which is challenging.

4.2 Ion production and collection

The collection of the radioactive ions after production in the target is under study at CRC, Louvain-la-Neuve, Belgium [11]. The development of the collection device for ^{8}Li is progressing and experiments are ongoing to measure the extraction efficiency. For the ^{8}B, due to its high reactivity, studies aim at finding suitable materials or possible compounds that can be extracted form the catcher.

Cross-section measurements for the reaction ^{7}Li(d,p)^{8}Li at the energies of interest have been done in INFN Napoli, Italy, in 2008 and data treatment is ongoing [10]. So far, the analysis confirms that the angular distribution of the ^{8}Li products has a maximum at around 8^o. The angular cross-section measurements for the ^{6}Li(^{3}He,n)^{8}B reaction are planned for 2011 at INFN Legnaro, Italy [24].

4.3 RF cavity

By traversing the 0.27 mg/cm^2 thick internal target, the Lithium ions will loose about 300 keV [4]. This energy has to be restored by an RF cavity. Since the revolution frequency is $\sim$ 3MHz, and the harmonic number should be as small as possible, a low-frequency cavity is needed. Moreover, the cavity should be as compact as possible, because of the space constraints.

The solution is to use an evacuated cavity with capacitive loading [25], in order to keep the size below 2m. A typical example at CERN is the bunch rotation cavity for ACOL (now

used in the AD) which reaches 750 kV at 9.55 MHz [26, 27]. It is a pulsed device dissipating 660 kW at full voltage. At 300 kV, operation in CW would be feasible.

The drawback of using such a cavity is that it requires good vacuum conditions to avoid multipacting. Indeed, the cavity needs 1 day conditioning before being put in operation.

A similar solution of a compact, low-frequency, high voltage, capacitive-loaded cavity has also been selected for the ERIT-FFAG, described in Sec. 4.6.

4.4 Charge exchange injection

Particles are injected in the ring as Li^{1+} ions at the gas-jet target location, which will also act as a stripper, and the circulating ions will be fully stripped. The transfer line and the injection have to be designed, however the design will be simpler than for standard H^-– injection systems, as the stripper will stay in the circulating beam being the target itself.

4.5 Beam scraper

In order to clean out large amplitude particles and have losses concentrated in one location, a beam scraper can be envisaged e.g. in the dispersive region opposite to the target.

4.6 The FFAG-ERIT experience

At Kyoto University, a prototype of a compact proton FFAG was built to produce neutron for Boron Neutron Capture Therapy (BNCT) via protons impacting on a Beryllium foil internal target [28, 29].

The FFAG-ERIT (Emittance Recovery Internal Target) makes use of the ionization cooling effect to reduce the transverse beam blow-up caused by Multiple Coulomb Scattering during target traversal. Thanks to its large (momentum) acceptance, it does not need longitudinal cooling. Parameters of the machine are very similar to the requirements of our Production Ring, since it stores protons at 11 MeV, has a mean radius of 2.35m and an RF cavity which provides a maximum voltage of 230kV at 18 MHz.

The project is closely followed-up and studies are ongoing [30] to investigate the possibility of using ERIT for the Beta-Beams production.

4.7 Target

In order to produce a sufficient number of beta-emitters per second, the gas-jet target density should be extremely high. Table 2 summarizes the specifications for the target, as from [4].

Existing gas-jet and cluster-jet target reach a maximum of 10^{15} atoms/cm^2, which is 4 order of magnitudes less than the thickness proposed in [4].

Examples of the performances of existing gas and cluster jet target is given in [31] and [32], the latter giving a comprehensive summary of jet and solid internal targets for accelerators.

Table 2: Gas-jet target [4].

Thickness	0.27	mg/cm^2
	5×10^{19}	atoms/cm^2
Diameter	5	cm
Density @ nozzle exit	~ 0.06	mg/cm^3
Pressure @ nozzle exit	250	Torr
Gas Volume (@ 250Torr)	4.3	m^3/s
Mach Number	4	
Nozzle throat	3.26	mm
Plenum Pressure	~ 3.5	atm
Length	~ 30	cm

The prototype for the H_2 cluster-jet target PANDA in FAIR, GSI, Germany, under development at Munster University, reaches a thickness of 8×10^{14} atoms/cm^2. The interesting feature for the Production Ring application, although density is not enough, is the possibility to have an adjustable shape for the target section, e.g. rectangular (can be triangular for our case), thanks to special laser-cut skimmers [33].

The H_2 gas-jet target in the Cooler ring at the Indiana University Cyclotron Facility [34] reaches 10^{16} atoms/cm^2, but the problem of a gas-jet is the background gas which is larger than for a cluster-jet.

Frozen-pellet targets, which are also under development at Munster University for PANDA [33], are not an option either, since the effective target thickness seen by the beam is of the order of 10^{15}/cm^2 as well.

The densities proposed in [4] can be reached in a gas-jet e.g for fusion application [35] or aerospace, but the critical issue for the Production Ring is to keep a good vacuum in the accelerator.

4.8 Vacuum issues

From the parameters in Table 2 it follows that the gas to be pumped out is:

$$Q = 250 \text{ Torr} \times 4.3 \text{ m}^3/\text{s} \approx 10^6 \text{Torr l/s} \tag{20}$$

Assuming we want to keep a pressure of 10^{-5} Torr, the pumping speed would be:

$$S = \frac{Q}{P} = 10^{11} l/s = 10^8 m^3/s \tag{21}$$

which is 3 order of magnitude higher than what an existing pumping system (even staged) can provide (see Appendix A, [36] and [31]).

Looking at the problem from the other side: if the maximum pumping speed is $S = 10^5$ l/s, the residual pressure around the target is:

$$P_{res} = \frac{Q}{S_{max}} = 10 \text{ Torr} \tag{22}$$

Assuming the entire beam pipe is coated by getters, they can remove another:

$$S_{getters} = s \times C \times 2\pi\, a = 30 l/s/cm^2 \times 10m \times 2\pi\ 10cm = 2 \times 10^6 l/s \tag{23}$$

but this means that the ring will be anyway at 1 Torr, which is an issue due to the vacuum constraints in the RF cavity.

5 Discussion of possible solutions

The required 10^{19}atoms/cm^2 thick gas-jet target in the accelerator vacuum environment represents the most crucial issue for the feasibility of the Production Ring.

Possible solutions have been investigated:

- Increasing the injected beam intensity, to reach the required ion production rate, is not feasible, since the proposed stable-ion sources are already at the limit of or beyond the available operational currents.
- Living with a poor vacuum in the machine, which could be a solution as long as the residual gas is "thin" with respect to the jet-target, causes multipacting in the RF cavity and it is therefore not feasible.
- Separating the target by "thin" windows causes a significant additional emittance growth and extra RF power to compensate for energy losses.
- Working at different energies is not an option, since 25 MeV is already the best compromise [4,10] between good production cross-section (which decreases with increasing energy) and stripping efficiency.
- Running with a "conventional" gas-jet target, with a 4 orders of magnitude lower thickness, decreases the production rate by the same amount. This is partly compensated by the increase in lifetime which will also increase the circulating beam current. The space charge limit is anyway at about 10^{12} ions/bunch therefore only a factor 10 can be gained. Moreover, since the energy lost and recovered in the RF cavity is smaller as well, the cooling rate (Eq. 9) is also lower by the same amount, therefore ionization cooling may not be efficient.
- Using CERN rings, such as AD, ELENA or LEIR, deserves feasibility studies. Since they are already existing, even if some upgrade is needed they will not contribute substantially to the cost of the facility, they have a larger circumference which allows the storage of a higher number of ions, for the same space-charge constraints, and they

are equipped with electron cooling, in case ionization cooling is weak. This solution is not as elegant as the one proposed in [4], but it may be considered if the production rates are high enough.

- Having a solid or liquid target allows to reach 10^{19}atoms/cm^2 target thickness. In this case it is preferable to have a Lithium target and a Deuterium or Helium beam (direct kinematic [17]). This is for the time being our preferred option and it is under study.

6 Conclusions

We have analyzed in detail the proposal by [4] to use a compact ring with an internal target to produce ^{8}Li and ^{8}B isotopes for the Beta-Beams.

A preliminary ring design is available. The optics studies have been done for the ^{7}Li(d,p)^{8}Li inverse kinematics case, but they can be easily scaled to the other reactions.

Due to the strongly negative slope of the Bethe Bloch function at the energies of interest for the isotopes production, the total budget of ionization cooling that can be achieved is very low, almost zero, therefore one should not expect sensitive emittance reduction but, in the best case, only control of the beam blow-up.

6D tracking tools are fully in place and predict what expected from analytical ionization-cooling considerations. SixTrack code allows us to see also the high order effects, e.g. chromaticity and second order dispersion, therefore the blow-up that is seen in the simulations is explained and could be corrected, although it is not so straightforward due to the small periodicity of the machine.

The lattice requires careful tuning to maximize ionization-cooling efficiency and in particular the beta function at the target position needs to be reduced as much as possible. Coupling with the vertical plane should be introduced as well.

Feasibility studies identified as a major issue the large thickness (10^{19}atoms/cm^2) required for the gas-jet target in a vacuum environment. The direct kinematics approach looks more feasible for the point of view of the target density, although the thin liquid-films technology (used as heavy-ions strippers and as target in nuclear physics) is still in early R&D [37].

7 Acknowledgments

Financial support of the European Community under the European Commission Framework Programme 7 Design Study: EUROnu, Project Number 212372 is acknowledged. The EC is not liable for any use that may be made of the information contained herein.

The author profited a lot from discussions, material and interest from many people. Among them: G. Arduini, E. Wildner, C. Hansen, E. Metral; D. Neuffer; M. Schaumann, T. Weber, J. Wehner; D. Kukler, K. Tinschert; R. Garoby; F. Caspers, M. Chanel, P. Chiggiato, O. Boine-Frankenheim, C. Dimopoulou, A. Khoukaz, A. Lehrach; V. Vlauchoudis,

C. Bracco, J. Barranco, V. Previtali, F. Schmidt, B. Holzer; Y. Mori, K. Okabe; E. Vardaci, V. Kravchuk, S. Mitrofanov.

A Brief recap about vacuum pumping

See also Ref. [36].
The quantity of gas can be measured in [pressure × volume] units since, at a given temperature T, the number of moles n is proportional to the pressure p and the volume V, via the ideal gas law:

$$pV = nRT$$

where $R = 8.3145$ J/mol K is the universal gas constant.
The gas throughput Q is measured in Torr l/s:

$$Q = P\frac{dV}{dt}$$

The pumping speed S is measured in l/s:

$$S = Q/P$$

Turbo-molecular pumps Turbo-molecular pumps work in a regime where the interaction between the molecules is smaller than the interaction with the wall (versus viscous pumps).

The maximum pumping speed that a mechanical pump can achieve is $S \sim 10^5$ l/s and there are constraints about the maximum ratio between the pressures inside and outside.

Cryogenics pumps and Getters Absorbing surface lifetime (the inverse of the molecules escape probability) is given by the *Frenkel equation*:

$$\tau = \tau_0 \exp \frac{E_0}{RT}$$

and it should be larger than the experiment duration. In order to extend τ, one can:

- increase the binding energy E_0 going to chemical bounds ⇒ getters: either in-situ deposition of evaporable getters like Ti-alloy or $BaAl_4$, either non-evaporable getters(NEG) coatings like TiZrV alloy, by heating up to some activation temperature

- reduce the temperature (to liquid Helium) ⇒ cryogenics pumps (nb, there you need to avoid contact of hydrogen with hydrogen, but need contact hydrogen with the metal, therefore you need porous materials with a high surface)

The maximum pumping speed for getters, assuming all coming molecules are pumped out, is $s = 44$ l/s/cm^2 for hydrogen. For heavier molecules it is worse since less molecules impact the surface and it goes as $\sim v\ 1/\sqrt{M}$. e.g. for Deuterium $s \sim 30$ l/s/cm^2.

References

[1] P. Zucchelli. A novel concept for a Neutrino Factory: the Beta-Beam. *Phys. Let. B*, 532:166, 2002.

[2] M. Benedikt et al. Conceptual design report for a Beta-Beam facility. *The European Physical Journal A - Hadrons and Nuclei*, 47:1–32.

[3] Euronu - A High Intensity Neutrino Oscillation Facility in Europe, FP7-INFRASTRUCTURES-2007-1.

[4] C. Rubbia, A. Ferrari, Y. Kadi, and V. Vlachoudis. Beam cooling with ionization losses. *Nuclear Instruments and Methods in Physics Research Section A: Accelerators, Spectrometers, Detectors and Associated Equipment*, 568(2):475 – 487, 2006.

[5] E. Fernandez-Martinez. The $\gamma = 100$ β-beam revisited. *Nuclear Physics B*, 833(1-2):96 – 107, 2010.

[6] V.V. Parkhomchuk A.N. Skrinsky. *Sov. J. Nucl. Phys.*, 12:3, 1981.

[7] D. Neuffer. Muon cooling. *Nucl. Instrum. Methods Phys. Res. A*, 532:26, 2004.

[8] M. Schaumann. Development and lattice design of an ion-production ring for a beta-beam facility. Bachelor Thesis, CERN-THESIS-2009-128, EUROnu-WP4-004, 2009.

[9] E. Benedetto. Ionization cooling in a low-energy ion ring with internal target for Beta Beams production. In *Proceedings IPAC'10*, 2010.

[10] E. Vardaci. Status of cross section measurements for ^{8}Li and ^{8}8B production, EUROnu-WP4-021, 2011.

[11] S. Mitrofanov. In *AIP Proceedings Nufact11*, 2011.

[12] Marrs et al. *PRC*, 8(427), 1973.

[13] Mc Clenahan et al. *PRC*, 11(370), 1975.

[14] C. Amsler et al. (Particle Data Group). *Physics Letters B*, 1(667), 2008.

[15] O. Boine-Frankenheim, R. Hasse, F. Hinterberger, A. Lehrach, and P. Zenkevich. Cooling equilibrium and beam loss with internal targets in high energy storage rings. *Nuclear Instruments and Methods in Physics Research Section A: Accelerators, Spectrometers, Detectors and Associated Equipment*, 560(2):245 – 255, 2006.

[16] D. Mohl. In *Proceedings CAS*, CERN-2005-004, 2005.

[17] D. Neuffer. Low-energy ionization cooling of ions for beta beam sources. *Nuclear Instruments and Methods in Physics Research Section A: Accelerators, Spectrometers, Detectors and Associated Equipment*, 585(3):109 – 116, 2008.

[18] E. Benedetto, M. Schaumann, and J. Wehner. Radioactive ions production ring for Beta Beams. In *Proceedings European Strategy for Future Neutrino Physics Workshop, CERN*, 2009.

[19] F. Schmidt et al. Sixtrack manual. CERN/SL/94-56 (AP), updated 2011.

[20] G. Robert-Demolaize et al. In *Proceedings 2005 Part. Accel. Conf., Knoxville*, page 4084, 2005.

[21] D. Kuchler. Private communication, 2009.

[22] K. Tinschert. Private communication, 2009.

[23] R. Iannucci K. Tinschert R. Lang, J. Bossler. Developement of a new high temperature oven for ECRIS. In *Proceedings. ECRIS'02*, 2002.

[24] V. Kravchuk et al. ^{8}B production measurements for the Beta Beam perspectives, CN Proposal, 2011.

[25] R. Garoby. Private communication, 2009.

[26] E. J. N. Wilson, editor. *Design study of an antiproton collector for the antiproton accumulator (ACOL)*. Number CERN 83-10. CERN, Geneva, 1983.

[27] J. Boucheron, R. Garoby, D. Gricr, M. Paoluzzi, and F. Pedersen. A 1 MV 9.5 MHz system for the CERN antiproton collector. CERN-PS-90-15-RF, 1990.

[28] Y. Mori. Development of FFAG accelerators and their applications for intense secondary particle production. *Nuclear Instruments and Methods in Physics Research Section A: Accelerators, Spectrometers, Detectors and Associated Equipment*, 562(2):591 – 595, 2006.

[29] K. Okabe, Y. Mori, and M. Muto. Recent studies of the FFAG-ERIT system for BNTC. In *Proceedings. PAC'09*, 2009.

[30] E. Benedetto. FFAG-ERIT for Beta Beam. 2011. (to be published).

[31] M. Macri. *Gas Jet Targets, CAS-Antiprotons for Colliding-beam facilities*. Number CERN-84-15. CERN, Geneva, 1984.

[32] C. Ekstrom. Internal targets for storage rings. *Nuclear Physics A*, 626(1-2):405 – 416, 1997.

[33] A. Koukaz. Presentation at CERN-GSI Meeting on internal targets, 2009. https://espace.cern.ch/betanu/MeetingsWP4/GSIMeeting291009/khoukazgsitargets.pdf.

[34] J. E. Doskow and F. Sperisen. Development of internal jet targets for high-luminosity experiments. *Nuclear Instruments and Methods in Physics Research Section A: Accelerators, Spectrometers, Detectors and Associated Equipment*, 362(1):20 – 25, 1995.

[35] V.A. Soukhanovskii et al. *Rev. Sci. Instrum.*, 75:4320, 2004.

[36] D. Brandt, editor. *CAS - CERN Accelerator School and ALBA Synchrotron Light Facility : Course on Vacuum in Accelerators*. CERN, Geneva, 2007.

[37] Y Momozaki, J Nolen, C Reed, V Novick, and J Specht. Development of a liquid lithium thin film for use as a heavy ion beam stripper. *Journal of Instrumentation*, 4(04):P04005, 2009.